23rd Australasian Conference on the Mechanics of Structures and Materials (ACMSM23)
Byron Bay, Australia, 9-12 December 2014, S.T. Smith (Ed.)

COMPRESSIVE STRENGTH AND STIFFNESS OF SENILE COCONUT PALMS STEM GREEN TISSUE

O.M. Gonzalez*
Griffith School of Engineering, Griffith University
Gold Coast campus, QLD, 4222, Australia. oswaldo.gonzalez@griffith.edu.au (Corresponding Author)

B.P. Gilbert
Griffith School of Engineering, Griffith University
Gold Coast campus, QLD, 4222, Australia. b.gilbert@griffith.edu.au

H. Bailleres
Salisbury Research Facility, Department of Agriculture, Fisheries and Forestry
Queensland Government, QLD, 4101, Australia. henri.bailleres@daff.qld.gov.au

H. Guan
Griffith School of Engineering, Griffith University
Gold Coast campus, QLD, 4222, Australia. h.guan@griffith.edu.au

ABSTRACT

The mechanical efficiency of a plant to resist external forces such as gravity (biomass), wind and rain water depends on the characteristic relationship between its form (morphology), material structure (anatomy) and function. Previous studies have shown that this relationship for coconut palms (monocotyledonous plant) significantly differs from hardwood or softwood (dicotyledonous plants) and even from other palm species. The coconut stem tissue (also referred to as "cocowood") has a non-uniform orientation of fibrovascular bundles and density distribution, likely influencing the coconut palm's mechanical properties and capacity to withstand extreme weather conditions without failure. The present study aims at quantifying and characterising the compressive strength and stiffness within the stem green tissue of senile coconut palms (80 to 100 year old) cut from the Pacific islands of Fiji and Samoa. This paper presents results gained from 69 compressive tests carried out on 54 green cocowood small-clear samples. Furthermore, this paper analyses the relationships between the measured mechanical properties and basic density.

KEYWORDS

Senile palm, cocowood mechanical properties, green tissue.

INTRODUCTION

Trees achieve mechanical efficiency essentially due to their unique anatomy that enhances their mechanical properties (Wegst, 2011). Palms are usually considered as natural structures that mechanically perform better than hardwood or softwood trees (Tomlinson, 2006), partially because of a superior hierarchical structure that maximises the biomechanical resistance, while minimising the amount of material used (Buehler, 2010; Gibson, 2012; Wegst, 2011). The coconut (*Cocos nucifera L.*) stem tissue, referred to as "*cocowood*" throughout this study (Gonzalez et al., 2014a), is a complex plant tissue that depicts a structure consisting of fibrovascular bundles and a ground tissue surrounding these bundles. The cells within the fibrovascular bundles are fibres with a honeycomb-like structure, while the ground tissue is made up of parenchyma with foam-like polyhedral cells (Butterfield et al., 1997; Gibson, 2012). The composition and structure of these elements, along with a high relative density of the fibrovascular bundles, give rise to high mechanical properties per unit mass. This in turn results in mechanically efficient natural structures (Gibson, 2012). This high mechanical performance is specifically observed in senile coconut palms, with the tall palm stem (greater than 25 metres) being able to withstand extreme weather conditions without failure. Studies towards understanding the orthotropic mechanical properties of cocowood are limited and mainly focused on estimating the modulus of elasticity (MOE) and bending modulus of rupture (MOR) in the longitudinal direction (L) (Bahtiar et al., 2010; Kuo-Huang et al., 2004). From an engineering perspective, better understanding the mechanical characteristics of this bio-material, not only in the L direction but also in the transverse (T) and radial (R) directions will provide foundation for potential biomimetic applications and future improvements of current engineered wood products (EWP).

MATERIAL AND METHODS

In this study, the strength and stiffness variation of coconut stem green tissue was mapped in terms of height and radial position. A total of 69 compressive tests were carried out on 54 green cocowood small-clear cubes, nominal size of 20 mm × 20 mm × 20 mm. The samples were selected from the complete set of cubes (4,066) cut during the ACIAR project FST/2004/054 (2010). The cubes were selected at three nominal heights of 0.2 m, 3.2 m and 9.4 m, and three radial positions corresponding to the core (low density, about 200 kg/m^3), mid-radial position (medium density, about 500 kg/m^3) and periphery (high density, about 850 kg/m^3). In total, the cubes were selected from 12 different palms. Six cubes were selected per height and radial position, therefore representing 9 sets of 6 samples each. Furthermore, the six cubes in a set were cut from three different palms and each set was therefore divided into 3 × 2 nominally identical samples. The method is similar to the "reconstruction method" used in Bahtiar et al. (2010). For each nominal elevation and radial position, three sets of data were collected, namely (i) the modulus of elasticity in the L (MOE_L) and R (MOE_R) (or T (MOE_T)) directions, (ii) the compressive modulus of rupture in the L (MOR_L) and R (MOR_R) (or T (MOR_T)) directions, and (iii) the Poisson's ratios in the LR (ν_{LR}), LT (ν_{LT}), TR (ν_{TR}) (or RT (ν_{RT})) directions. Only the compressive MOE and MOR are reported in this paper. The Poisson's ratios can be found in Gonzalez et al. (2014b). For each group of nominally identical cubes, the first cube was tested in the L direction to obtain the MOE_L and MOR_L, and the second cube was tested in the T (or R) direction to obtain the MOE_T and MOR_T (or MOE_R and MOR_R). Care was taken to have the fibrovascular bundles parallel to the cube longitudinal axis, with a +/- 5º tolerance. Before testing, samples were sanded to guarantee flat surfaces and saturated with water to reproduce green conditions. The samples preparation methodology is detailed in Gonzalez et al. (2014b). In the test, 5 mm strain gauges were glued to the samples in the L, T and/or R directions (Gonzalez et al., 2014b) and the strain was recorded in the parallel and perpendicular directions to the load. The tests were carried out in a 30 kN Lloyd universal testing machine at a constant displacement rate to reach failure between 3 to 5 mins. The lower platen was fixed while the upper platen was mounted on a half sphere bearing which could rotate, so as to provide full contact between the platen and the samples. To minimise friction, dry lubricant (graphite powder) was used between the samples and the testing platens. Figure 1 details the experimental set-up and strain gauge positions.

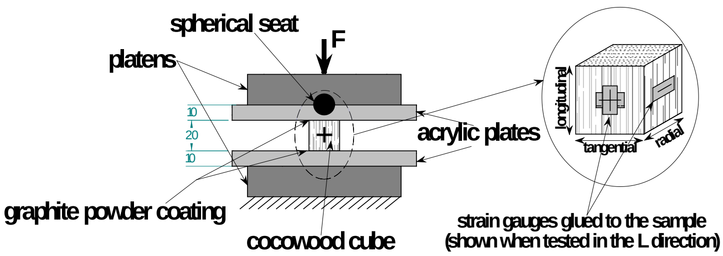

Figure 1. Compressive sample test set-up

RESULTS

Green modulus of elasticity (MOE)

The compressive stress (σ_i) applied to the sample is calculated as,

$$\sigma_i = F / A \tag{1}$$

where F is the recorded applied load, i denotes the direction of loading (i.e. L, T or R) and A is the cross-sectional area of the sample's face perpendicular to the force F. Figure 2 plots typical recorded stress-strain curves for two nominally identical samples loaded in the L (Fig. 2(a)) and T (Fig. 2(b)) directions. The samples were cut at 3.2 m and at the periphery of the palm. As friction was limited between the samples and the platens, no stress developed in the plane perpendicular to the load and the Hooke's law (Ugural, 2008) applies. The stress-strain relationship is then given as,

$$\sigma_i = MOE_i \cdot \varepsilon_{ii} \qquad (2)$$

where MOE_i and ε_{ii} are the MOE and strain, respectively, in the *i* direction of loading.

The modulus of elasticity is a measure of the elastic stiffness of the material. The cocowood MOEs in the three principal directions are calculated by performing a linear regression on the linear part (proportional limit) of the stress-strain curves, as shown in Figure 2.

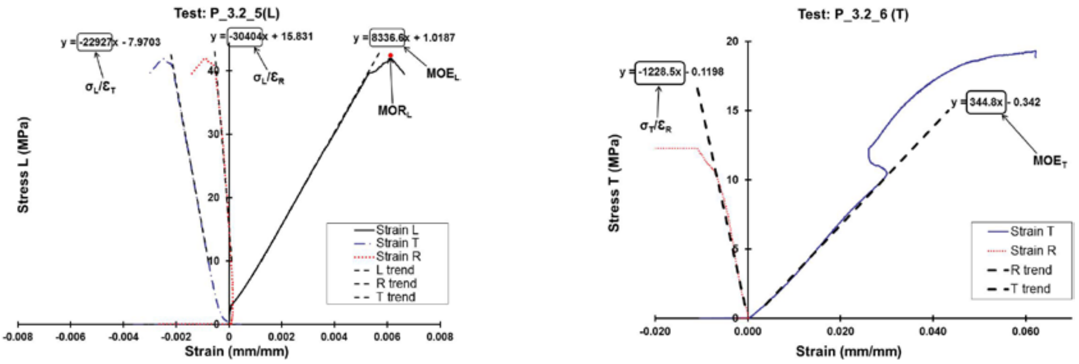

(a) (b)

Figure 2. Stress-strain curves when the compressive load is applied in the (a) L and (b) T directions

Due to the upper platen still adjusting at the beginning of the tests, full contact between the upper platen and the specimens was usually not fully achieved during this phase. The initial non-linear part was therefore disregarded when calculating the MOE, as shown in Figure 2.

Figure 3 plots all measured MOEs against the measured basic density, i.e. the oven-dry weight divided by the green volume, in the three loading directions. A strong correlation ($R^2 > 0.96$) exists between the green MOE and basic density. Similar to the density distribution pattern within the coconut stem (Gonzalez et al., 2014a), the green MOE would therefore decrease "sigmoidally" from the periphery to the core and mostly linearly with the palm elevation. The green MOE in the L direction is 9 to 26 times greater than the green MOEs in the T and R directions. Green MOEs in the T and R directions are of similar values, with the green MOE in the T direction tending to be lower (up to 25%) than the same in the R direction. No clear correlation can be found between the green MOE and the palm elevation, despite the diameter of the fibrovascular bundles decreasing with the elevation for samples of same density. Based on results presented in Figure 3, the following equations are proposed to map the green MOE (in MPa) in the L, R and T directions as a function of the basic density *d* (in kg/m³),

$$MOE_L = 10.4d - 967.26\,, \qquad MOE_R = 0.55d - 36.13\,, \qquad MOE_T = 0.38d + 2.26 \qquad (3)$$

The basic density is mapped in Gonzalez et al. (2014a) in terms of palm elevation and radial position.

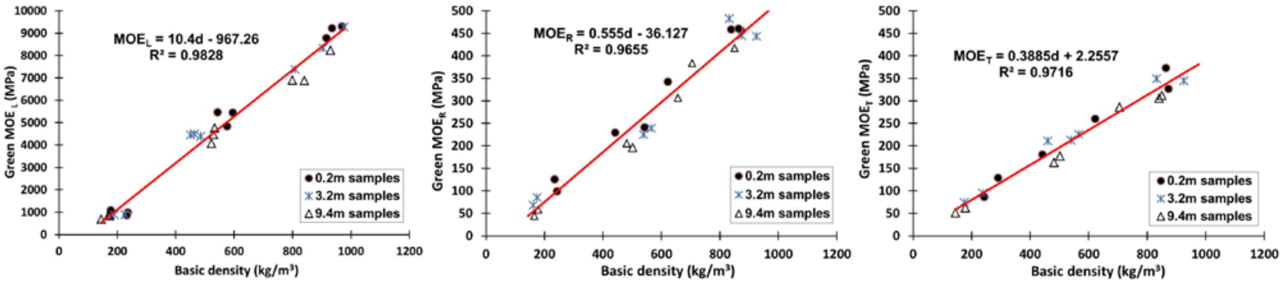

(a) (b) (c)

Figure 3. Green MOE-basic density relationships in the (a) L, (b) R and (c) T directions

Green modulus of rupture (MOR)

When tested in the L direction, the load always reached a maximum and the compressive MOR_L parallel to the fibre is given as (DIN EN 408, 2003),

$$MOR_L = F_{max} / A \tag{4}$$

where F_{max} is the maximum applied load and A is the cross-sectional area of the sample's face perpendicular to the load F.

When the load was applied perpendicular to the fibre (in the R or T directions), no maximum load was reached after a plastic deformation greater than five times the elastic deformation. This mechanical behaviour is commonly encountered in bio-materials (Gibson, 2012). The compressive strength was then calculated in accordance with the European Standard EN408 (DIN EN 408, 2003; Leijten et al., 2012) and defined as the intersection between the stress-strain curve and a line parallel to the elastic part of the curve with 1% strain offset. Figure 4 illustrates this procedure for a sample tested along the R direction, in which the intersection of the stress-strain curve and the line occurs at a stress equal to 17.2 MPa.

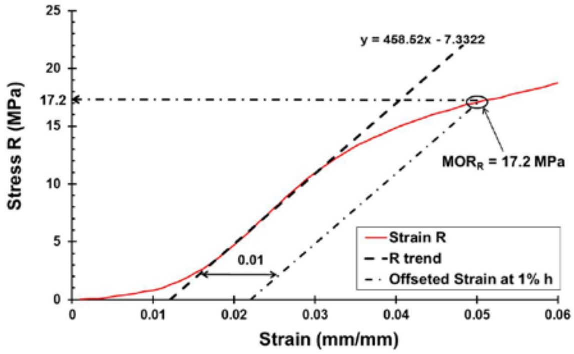

Figure 4. Green MOR from a sample tested perpendicular to the fibre

Figure 5 plots all measured MORs against the measured basic density of the samples in the three loading directions. A strong correlation ($R^2 > 0.98$) exists between the green MOR and basic density.

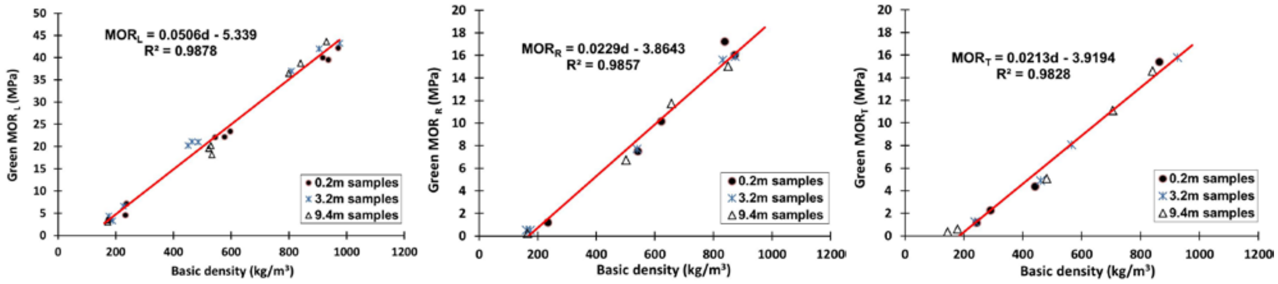

Figure 5. Green MOR-basic density relationships in the (a) L, (b) R and (c) T directions

Similar to the basic density distribution pattern (Gonzalez et al., 2014a), the MOR would also decrease "sigmoidally" from the periphery to the core and mostly linearly with the palm elevation. Similarly to the MOE, no clear correlation was found between the green MOR and the palm elevation. The green MOR in the L direction is 3 to 6 times greater than the green MORs in the R and T directions. The green MOR in the T direction is usually lower (up to 50%) than the same in the R direction. Based on the results presented in Figure 5, the following equations are proposed for the green MOR (in MPa) in the L, R and T directions as a function of the basic density d (in kg/m^3),

$$MOR_L = 0.051d - 5.34, \quad MOR_R = 0.023d - 3.86, \quad MOR_T = 0.022d - 3.92 \tag{5}$$

Figure 6 plots the relationship between the green MORs and MOEs in the three principal directions. As shown in the figure, there is a strong linear correlation ($R^2 > 0.95$) between the two values in all tested directions.

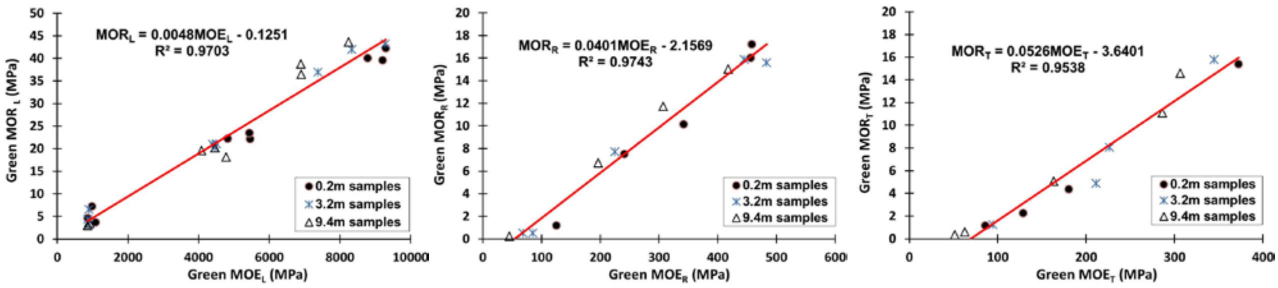

(a) (b) (c)

Figure 6. Green MOE-MOR mutually interdependence in the (a) L, (b) R, (c) T directions

From Figure 6, the following equations between the green MOE and MOR (both in MPa) in the L, R and T directions can be proposed,

$$MOR_L = 0.0048MOE_L - 0.13\,, \quad MOR_R = 0.040MOE_R - 2.16\,, \quad MOR_T = 0.0526MOE_T - 3.64 \qquad (6)$$

DISCUSSION

The research outcomes of this study show that the green cocowood strength and stiffness can be solely expressed as a function of the basic density. Using the basic density distribution within a characteristic coconut palm stem proposed in Gonzalez et al. (2014a), the green cocowood mechanical properties can also be mapped within the entire coconut stem. To illustrate this, the distribution of the MOE in the L direction is mapped in Figure 7 for a characteristic 25 m high senile coconut stem.

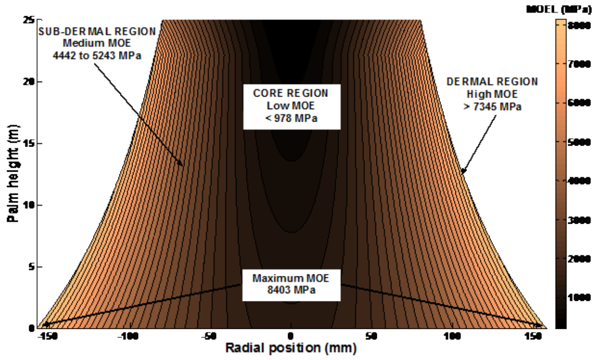

Figure 7. Green MOE_L distribution within a characteristic coconut palm

As shown in Figure 7, in a characteristic coconut palm, the green MOE_L at the palm stem core region would linearly decrease from 1,352 MPa at the bottom to 198 MPa at the top. At the coconut palm stem periphery, it would linearly decrease from 8,403 MPa at the bottom (maximum value of MOE_L) to 7,394 MPa at 22 m height, and then further linearly decrease to 5,221 MPa at the top (25 m). Based on Eqs. (3) to (5) and the proposed distribution of basic density in Gonzalez et al. (2014a), Table 1 gives characteristic green MOE values in the L, R and T directions at specific locations of the coconut palm. As shown in Table 1 and Figure 7, the characteristic MOE values encountered in cocowood are highly heterogeneous. In the R and T directions, they span from 26 MPa to 464 MPa and from 46 MPa to 352 MPa, respectively. Similar calculations are conducted for the green MOR in the L, R, and T directions and are also given in Table 1. Green MOR characteristic values range from 0.3 MPa to 40 MPa in the L direction, from 0 to 16.8 MPa in the R direction and from 0 to 15.3 MPa in the T direction.

Table 1. Calculated green MOE and MOR variation for a characteristic coconut palm

Palm's location	Radial position	Basic Density (kg/m3)	MOE_L (MPa)	MOE_R (MPa)	MOE_T (MPa)	MOR_L (MPa)	MOR_R (MPa)	MOR_T (MPa)
Bottom (0 m)	Periphery	901	8403	464	352	40.3	16.8	15.3
	Core	223	1352	88	89	5.9	1.2	0.8
Top (25 m)	Periphery	595	5221	294	233	24.8	9.8	8.8
	Core	112	198	26	46	0.3	0.0	0.0

CONCLUSIONS

This study quantifies and characterises the strength and stiffness along the stem green tissue of senile coconut palms cut from Fiji and Samoa islands. Specifically, a total of 69 compressive tests were carried out over 54 green cocowood small-clear samples to determine the Modulus of Elasticity (MOE) and compressive Modulus of Rupture (MOR). Furthermore, this paper analyses the relationships between the measured mechanical properties and basic density. Simple equations are proposed describing the characteristic distribution patterns of the cocowood mechanical properties within the palm's stem as a function of the basic density distribution.

The mechanical properties were found to be linearly proportional to the basic density and therefore vary similarly to the latter within the palm stem tissue. They consequently decrease from the periphery to the core, and from the bottom to the top of the palm. The characteristic green MOEs were found to vary from 198 to 8,403 MPa, 26 to 464 MPa, and 46 to 352 MPa, in the L, R and T directions, respectively. The characteristic green MOE in the L direction was found to be 9 to 26 times greater than the ones in the R and T directions. The compressive characteristic green MORs were found to vary from 0.3 to 40 MPa, 0 to 17 MPa, and 0 to 15 MPa, in the L, R and T directions, respectively. The characteristic green MOR in the L direction was found to be 3 to 6 times greater than the ones in the R and T directions. The characteristic green MOR in the T direction was found to be usually lower (up to 50%) than the same in the R direction. The MOE and the MOR were found to be linearly correlated in all directions.

ACKNOWLEDGMENTS

The authors thank the Department of Agriculture, Fisheries and Forestry (DAFF), Queensland Government, for supplying the cocowood samples for conducting the experimental tests. Mr Rodney Vella is specially acknowledged for providing direct support during the preparation of the samples.

REFERENCES

ACIAR project FST/2004/054 (2010). "Improving value and marketability of coconut wood." Australian Centre for International Agricultural Research, Australia.

Bahtiar, E., Nugroho, N., and Surjokusumo, S. (2010). Estimating Young's Modulus and Modulus of Rupture of Coconut Logs using Reconstruction Method. *Civil Engineering Dimension* 12, 65-72.

Buehler, M. J. (2010). Tu (r) ning weakness to strength. *Nano Today* **5**, 379-383.

Butterfield, B. G., Meylan, B. A., and Peszlen, I. M. (1997). "Three dimensional structure of wood," Hungarian/Ed. Chapman and Hall Ltd, London.

DIN EN 408 (2003). Determination of some physical and mechanical properties of structural timber and glued laminated timber. Vol. EN 408 : 2003, pp. 29. European Committee for Standarization, Brussels.

Gibson, L. J. (2012). The hierarchical structure and mechanics of plant materials. *Journal of The Royal Society Interface* 9, 2749-2766.

Gonzalez, O. M., Gilbert, B. P., Bailleres, H., and Guan, H. (2014a). Senile coconut palm hierarchical structure as foundation for biomimetic applications. *Applied Mechanics and Materials - Advances in Computational Mechanics* 553, 344 - 349.

Gonzalez, O. M., Gilbert, B. P., Bailleres, H., and Guan, H. (2014b). "Understanding senile coconut palms as foundation for biomimetic applications - part II: mechanical properties of stem tissue," Rep. No. OMG/2014/R02. Griffith University, Griffith School of Engineering.

Kuo-Huang, L. L., Huang, Y. S., Chen, S. S., and Huang, Y. R. (2004). Growth stresses and related anatomical characteristics in coconut palm trees. *IAWA Journal* 25, 297-310.

Leijten, A., Franke, S., Quenneville, P., and Gupta, R. (2012). Bearing Strength Capacity of Continuous Supported Timber Beams: Unified Approach for Test Methods and Structural Design Codes. *Journal of Structural Engineering* 138, 266-272.

Tomlinson, P. B. (2006). The uniqueness of palms. *Botanical Journal of the Linnean Society* 151, 5-14.

Ugural, A. C. (2008). "Mechanics of Materials," John Wiley & Sons Inc, New Jersey Institue of Technology, United States of America.

Wegst, U. G. K. (2011). Bending efficiency through property gradients in bamboo, palm, and wood-based composites. *Journal of the mechanical behavior of biomedical materials* 4, 744-755.